Dispersive Granular Flow in a Horizontal Drum Stirred by a Single Blade

B. F. C. Laurent and J. Bridgwater
Dept. of Chemical Engineering, University of Cambridge, Cambridge, CB2 3RA, U.K.

To understand the detailed processes occurring in stirred systems for particulate materials, experiments were conducted in a horizontal cylindrical mixer, 270 mm dia. and 650 mm long. It was stirred by a single long flat blade, varying the level of fill between 20 and 70% and the agitator speed between 20 and 45 rpm. The dispersion of blobs in three regions — in the transaxial plane near the wall, in the path of the blade, and in the bulk — suggested two classes of behavior. The dispersive behavior of particles was characterized by axial dispersion coefficients and root mean-square radial displacements, parameters commonly useful for process design. Both parameters showed that powder flow was independent of blade speed and controlled by the number of blade passes. Agitation was nonuniform in the transaxial plane with two regions of enhanced axial and radial displacement. These occurred near the free surface and immediately beneath the region where the blade arm was horizontal so that material readily slides off the blade. The axial dispersion coefficient was a maximum at a fill level of 40%, contributing effects arising from the free surface area of the bed and the conveying capacity of the blade.

Introduction

Although mixing of powders is common in industrial processes, the mechanisms governing flow patterns are not well understood. This is in contrast to, say, liquid mixing where considerable knowledge exists. The influence of operating parameters on flow patterns in powder systems is generally not known either in the laboratory or in the industrial scale. The traditional form of investigation is to conduct experiments in a laboratory-scale mixer, but scale-up to pilot and then to industrial scale is difficult due to great uncertainties about employing dimensional analysis in a proper manner.

Theoretical models of powder mixing have been based on a statistical approach. For instance, Müller and Rumpf (1967) developed such a model and applied it to experiments. However, due to a lack of powerful experimental techniques, the general development of models describing particle flow patterns has not been possible until now. Thus, the existing models are of very limited value.

Considerable efforts have been made recently to simulate particle mixing. One example is that of Khakhar et al. (1999) who examined particle flow in two-dimensional (2-D) mixers of circular, elliptical, and square cross-section. They modeled the deformation of circular blobs situated in various portions of the cross-section and checked their predictions experimentally using particle velocimetry. Their findings showed that either dispersive mixing or chaotic mixing could arise; theory and experiments were in accord. Work using the discrete element method performed by Kaneko et al. (2000) on a mechanically stirred chemical reactor where polymerization takes place gives another idea of the progress achieved in the numerical simulation of discrete particle systems. An overview of current research in this field has recently been given (Thornton, 2000).

Noninvasive techniques have recently provided a great deal of information on 3-D flow of granular material, in particular with the rapid development of tomographic techniques (Williams and Xie, 1993). These represent a considerable achievement compared to methods of investigation such as particle velocimetry; the work of Malhotra et al. (1990) provides an illustration of the latter by using such a technique on a mechanically stirred powder dryer.

The studies of Laurent et al. (2000) established the flow patterns occurring in one particle mixing system of industrial interest, yet of sufficient simplicity to perceive and understand the structure of the flow. Their work examined the spa-

tial distribution of the material and the velocity profiles. However their imaging data can further be used to provide detailed information to build into a model of equipment behavior such as a chemical reactor or a dryer. Here, the effects of dispersion, a central issue in unit operations, are evaluated both along and across a mixer.

Experimental Method

The mixing chamber (Figure 1) is a fixed horizontal cylinder of internal diameter 270 mm and of length 650 mm stirred by a simplified version of an industrial agitator featuring six series of three radial supports fixed onto the 90 mm diameter rotor shaft. The set of radial supports defines five compartments in the axial direction; one of the three radial supports at each axial position was used to hold a single long flat blade along the length of the mixer. The plane of the blade is inclined to 45° to the radial direction. The clearance between the tip of the blade and the inside of the cylindrical shell is 8 mm, and that between the blade tip and the inside of the end of the shell is 4 mm. The powder used had a bulk density of about 500 kg/m^3 and an internal angle of friction of 30°. The internal angle of friction and the angle of repose are equal in the present case, since the material is cohesionless. The shape of the particle was approximately spherical and its specific density was about 0.91 kg/L. The mean particle diameter, as measured by sieving, was 520 μm and the standard deviation of the size distribution was 90 mm.

The work uses positron emission particle tracking (PEPT). This noninvasive method of investigating liquid or solid systems provides vastly more information on powder flow patterns than other methods commonly used such as sampling. In PEPT the motion of a single positron-emitting tracer is followed in the three dimensions, with the position of the tracer being obtained 10–20 times per second. This frequency is not constant and depends upon the strength of the radioactive tracer, the size of equipment, and the tracer speed as fully discussed by Parker et al. (1993). The output is a data file containing the spatial co-ordinates of the tracer as a function of time. Particles moving at up to 2 m/s can be followed. The uncertainty in three dimensions or spatial resolution is approximately 2 mm for a speed of 0.2 m/s and increases with the speed of the positron emitter to about 5 mm at a speed of 1 m/s. The tracer used here was a 0.6 mm diameter resin particle containing absorbed water with ^{18}F atoms produced by bombarding the water with ^{3}He ions. The tracer had a diameter of 600 μm and a specific density of about 1.04 kg/L, that is, close to that of the bulk particles, with its motion thus representing the behavior of the bed.

Results and Discussion

Transaxial flows

General Description of the Flow. Here, the general flow structure is first presented. The agitator yields different flow patterns at a low and a high level of fill, which are sketched qualitatively in Figure 2 (Laurent et al., 2000). This shows the direction of the most significant displacements for a specific blade position and the approximate position of stationary zones. At a low level of fill, the free surface of the bed does not interfere with the rotating shaft (Figure 2a). As the blade penetrates into the particle bed, the material is pushed forward and the inclination of the free surface increases. A void is created behind the blade. As the blade progresses further, the material is progressively lifted by the blade, also forming a circulation loop over the top of the blade. As the blade moves out of the bed, the material cascades off the blade and rolls down the free surface. When the blade is out of the bulk, the particle bed is at rest and the free surface defines an angle observed to be lower than the angle of repose.

The free surface of the bed first touches the agitator shaft when the level of fill is 33%. At higher levels of fill, the agitator shaft interacts with the bed and inhibits radial motion, forcing the material to move around the shaft and to flow through the annular space between the shaft and the mixer shell (Figure 2b). Most of the material convected by the blade then flows over the agitator shaft, although some still flows under the shaft. The material is lifted out of the bed by the blade and then falls onto the free surface. The region of the bed over the top of the blade where a loop of circulation forms is now found closer to the agitator shaft.

Earlier observations concluded that the flow in this system is essentially confined to the transaxial plane. Indeed, the standard deviation of the axial velocity was observed to be about ten times lower than that of the radial and tangential velocity, inferring weak axial flow compared to transaxial flow. This is an important result confirming the findings of Metcalfe and Shattuck (1996). Using NMR visualization in horizontal rotating drums, they noted that radial dispersion was around ten times higher than axial dispersion. The results

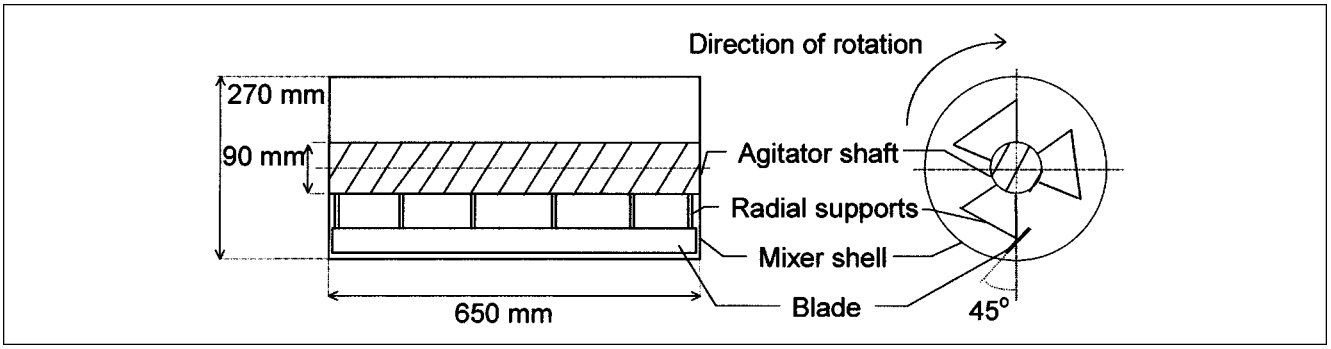

Figure 1. Mixer: side and cross-sectional views.

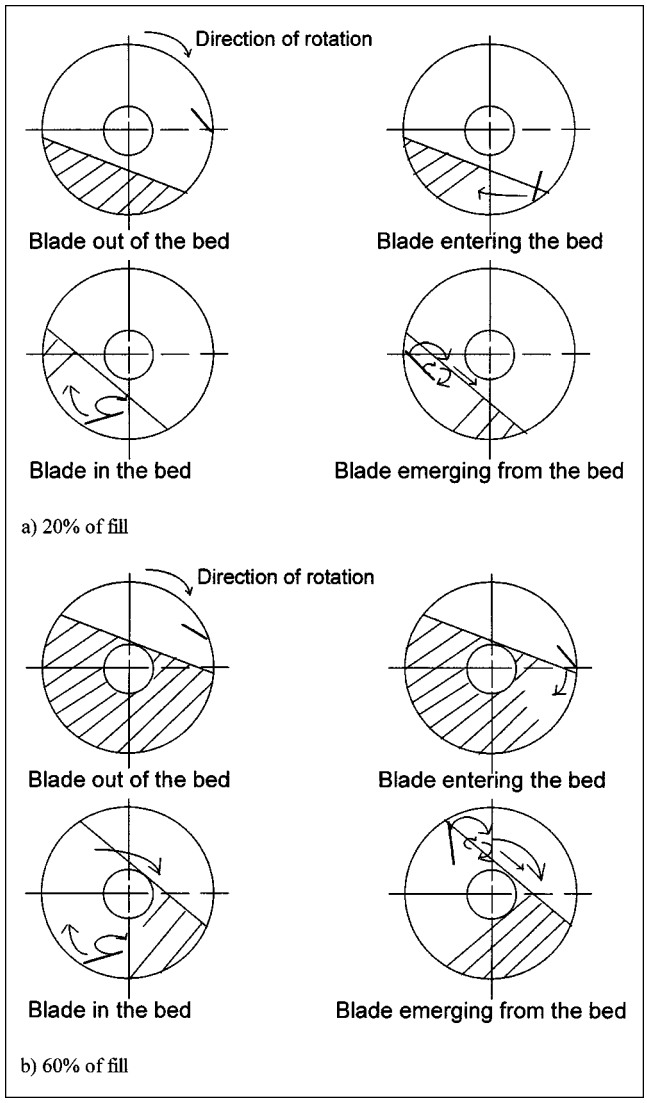

Figure 2. Blade cycle; transaxial flow patterns.

Striped zone is stationary.

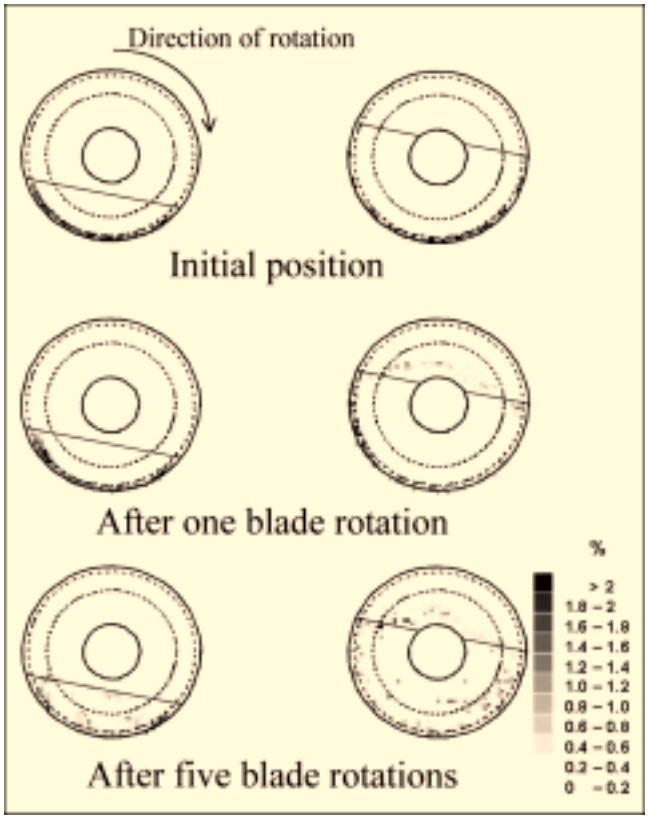

Figure 3. Radial dispersion of a labeled slice in the clearance between the tip of the blade and the outer wall.

Left column: 20% of fill; right column: 60% of fill; $N = 38$ rpm.

found in the present case justify the use of the analysis developed by Khakhar et al. (1999) to describe 2-D periodic flows.

Deformation of Blobs. To describe flow, software reconstructs from the data file the deformation of a labeled region, or a blob, in the transaxial plane after a number of blade rotations. A particular region of interest in the transaxial plane is chosen, as well as a number of blade rotations and the associated time. Data points situated in the blob are selected from the data file, while the blade is out of the particle bed, ensuring that the bed is initially in a state of rest or nearly so. An initial point is defined by any data point satisfying these conditions; let it be selected from the data file at time t_i where the subscript is the reading in the sequence of data points. The subsequent motion of the tracer, starting from each initial point, is tracked; the spatial position of the tracer, the chosen number of blade rotations, and the associated time defines a data point called a final point. The transaxial plane is divided into a grid of 5 mm by 5 mm bins, and the bin in which the final point exists is determined. The final position of points situated initially in the original blob is mapped in the transaxial plane and is called "deformed blob." The scale gives the ratio of the number of initial points found in a bin after n blade passes to the total number of points found in the initial blob. In order to take into consideration the nonconstant sampling rate arising from the slow decay of radio-activity, each final point is weighted by $(t_{i+1} - t_{i-1})$, the time interval between the two points adjacent to the initial point in the data file. As a summary, the tracking technique collects data in a Lagrangian form. These are then converted into Eulerian coordinates. This is possible because the Lagrangian results arise from a flow field which is steady, that is, a field averaged over a blade cycle. What is obtained is an Eulerian plot.

Three radial zones were selected to reveal details of the mechanisms influencing the flows in the transaxial plane, the transaxial area being the same for each blob. Although the data are integrated over the mixer length (which makes the volume the same for all three blobs), it does not imply that the number of data taken from PEPT is the same. The two dotted lines on each plot (Figures 3, 4 and 5) mark the loci of the tip and the rear of the blade as the blade rotates. The position of the free surface is given by the inclined lines on the figures.

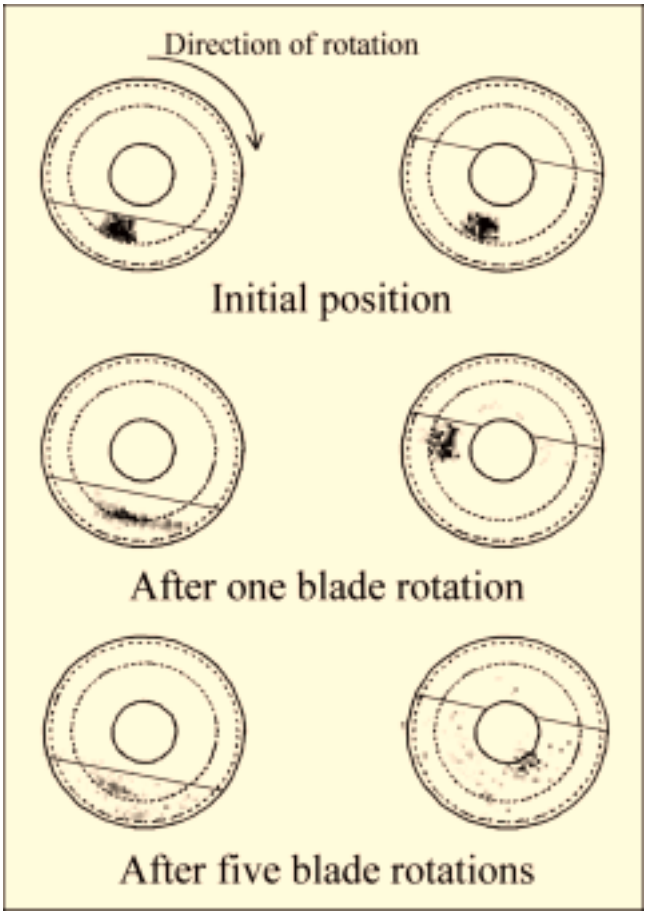

Figure 4. Radial dispersion of a labeled slice in the central part of the bed beneath the agitator shaft.

Left column: 20% of fill; right column: 60% of fill; $N = 38$ rpm.

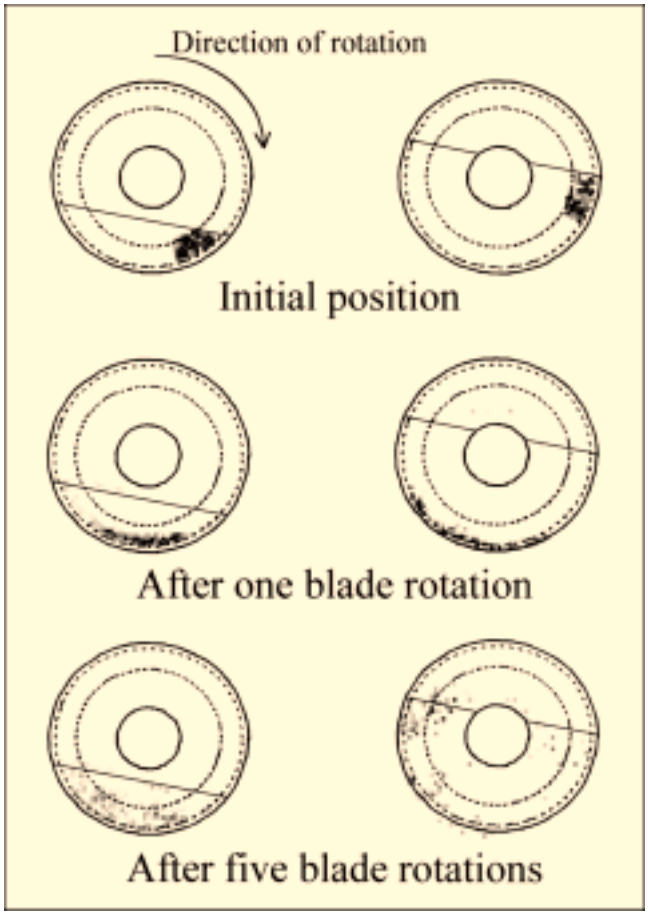

Figure 5. Radial dispersion of a labeled slice in an annular section in the path of the blade.

Left column: 20% of fill; right column: 60% of fill; $N = 38$ rpm.

The first region is situated between the tip of the blade and the inner surface of the mixer chamber. Figure 3 shows the dispersion of a labeled portion of an annulus of particles of 5 mm width with its outer surface situated at the external surface of the particle bed, essentially the clearance between the blade tip and the wall. For both levels of fill, the labeled material progressively reaches the free surface. At 20% of fill, the dispersion of the material in the clearance region is a slow process in both the radial and the angular directions (Figure 3, left column) and increases with level of fill (Figure 3, right column). These observations are in agreement with Malhotra et al. (1990) who studied transaxial powder flow through the end wall of a cylindrical mixer (diameter 250 mm, length 150 mm) stirred by a single paddle. They measured the circumferential displacement of colored tracers situated in the clearance zone as a function of the number of blade passes and showed that the residence time in the clearance region decreased with increase of fill, indicating that particle displacement in the clearance region increases with fill.

The second region is a portion of the annular space between the agitator shaft and the radius defined by the inner tip of the blade. Figure 4 shows the deformation of this labeled region for both 20% and 60% of fill. After one blade rotation, the blob is stretched along the direction of the flow; some material has fallen into the region where the blade passes. A region of higher occupancy appears near the center of the circulation loop sketched in Figure 2a. After five blade rotations, most of the labeled powder has been dispersed in the transaxial plane; the region of higher occupancy mentioned earlier remains. At 60% of fill, the labeled region is less elongated than at a lower level of fill and has been pushed towards the free surface after one blade rotation (Figure 4, right column). Note that locations situated in the shaft region are artifacts arising from the reconstruction of the dispersion provided by the software. After five blade rotations most of the labeled powder is observed to have moved over the agitator shaft, but is less dispersed radially than at lower fill levels. This arises because the material slumps down the free surface without the direct action of the blade. The flow pattern is more regular, that is, showing streamlines more nearly closed as opposed to the streamlines at low fill which are disturbed by the blade pass.

The third region is that portion of the annulus having the same width as the blade lying beneath the free surface in the annular region directly in the path of the blade. At 20% of fill and after one blade rotation (Figure 5, lefthand column),

the labeled powder is pushed forward along the blade path. After five blade rotations, the labeled powder is mostly situated in the region where the blade interacts with the bed. The powder is convected by the blade and falls progressively into a relatively open space behind the moving blade. At 60% of fill, the labeled powder is, after one blade rotation, less dispersed in the circumferential direction. Little material has been pushed towards the rotating shaft, and most of it has been pushed towards the outer wall. This may be explained by the increased downward forces due to gravity caused by the increased overburden of material and the action of the blade. After five blade rotations, most of the labeled powder is pushed towards the top of the free surface. Little material has been pushed over the agitator shaft.

At 20% fill and after five blade revolutions, close observation of Figures 3 and 5 suggests that the pictures may well be similar, implying that flow originating in both initial blobs may be of the same nature. Examination of Figure 4 shows a different behavior, the images possibly being the reverse from each other. This argument may be extended to higher fill level although the reduced amount of data lends less confidence to the conclusion.

These results suggest the possibility of two regions of different topological nature coexisting in the transaxial plane. The work by Khakhar et al. (1999) on transaxial mixing in rotating drums suggests that the first region, limited by the rear of the blade and the inner mixer wall, is of chaotic nature. The second, situated above the other and separated from the other by an invariant curve, also called KAM curve (Ott, 1993), is of regular nature. From the geometry of the system, it is thought that such a KAM curve would be approximately situated on the dotted line marking the locus of the rear of the blade. These preliminary considerations need to be checked formally, for instance, by further investigations to validate the hypothesis of the presence of an invariant curve.

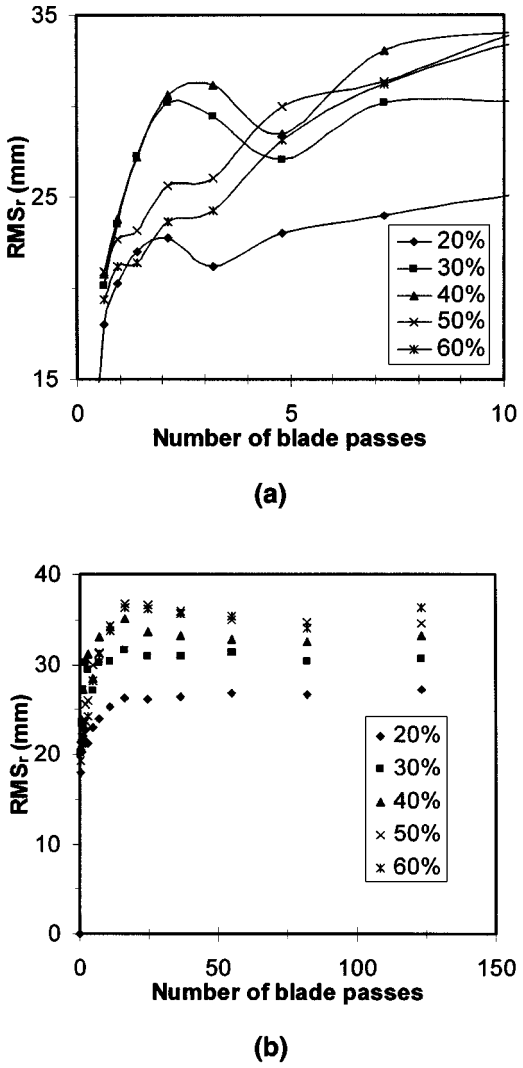

Figure 6. Root mean square of the radial displacement RMS_r vs. number of blade passes, influence of the level of fill; $N = 38$ rpm.

(a): 0 to 10 blade passes; (b): 0 to 150 blade passes.

Radial displacement

The trajectory of the particles follows an orbital path, particles rotating either around a circulation loop beneath the agitator shaft or flowing over it (Figure 2). This suggested the use of the root mean square of the radial displacement RMS_r, which quantifies the ability of the tracer to change orbit. Analysis of PEPT results gives direct access to RMS_r. The motion of the tracer is tracked for each data point and the radial displacement of the tracer is calculated as a function of a time t. The square of the radial displacement for all the data points is then averaged and leads to RMS_r for the given time t.

Figures 6a and 6b show the influence of the level of fill on RMS_r as the number of blade passes is varied. Figure 6a features RMS_r after a short number of blade passes, that is, directly related to the dynamic of the bed, whereas Figure 6b shows the evolution of the system as it reaches asymptotically its steady state. RMS_r first increases with the number of blade passes (Figure 6a), but then decreases after about five blade passes for 30% and 40% fill. Furthermore, RMS_r rises most rapidly when the level of fill is 30% or 40%. The behavior after a small number of blade passes suggests that RMS_r is a maximum for 40% of fill, implying that radial displacement is greatest at 40% fill after a small number of blade passes, approximately seven. This suggests the existence of a transition period starting around 30% fill as the free surface starts intersecting the agitator shaft. During this transition period, particles may either flow over the agitator shaft or roll underneath it in the circulating loop sketched in Figure 2b. This bifurcation enhances the radial dispersion, which is here the ability for particles to change orbital path and is thought to be maximum around 40% of fill, as shown by the RMS_r maximum for 40% fill. The bifurcation decreases in intensity with increase of fill as most of the material then flows over the agitator shaft. RMS_r then reaches a limit after about 50 blade passes (Figure 6b). This limit is an increasing function of the level of fill as allowed by the displacements permissible due to the geometry of the bed as the cross-sectional area of the bed increases with fill.

We can readily calculate the limit of RMS_r for the case where a tracer starting from any point in the cross-sectional

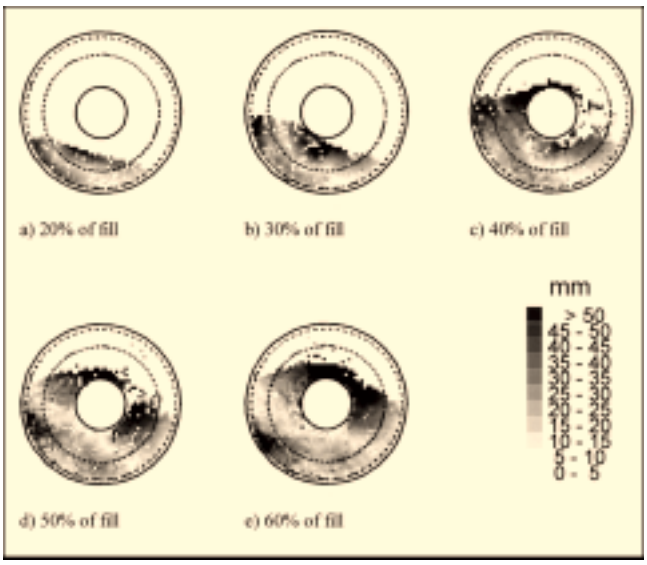

Figure 7. Root mean square of the radial displacement RMS_r after one blade rotation; $N = 38$ rpm.

The white bins are those where the number of data points was insufficient (less than twenty) to calculate RMS_r.

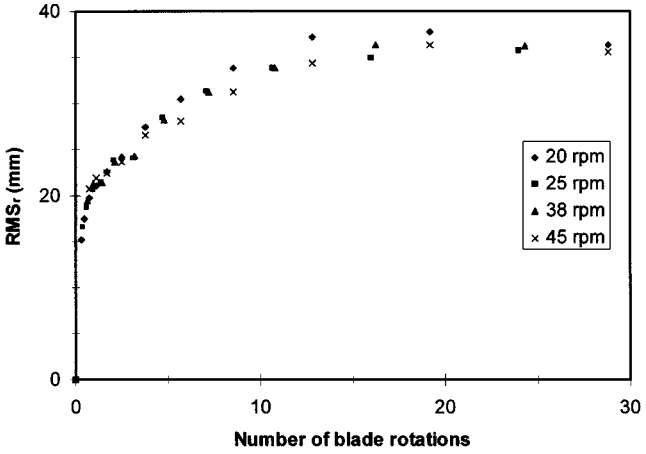

Figure 8. Root mean square of the radial displacement RMS_r vs. number of blade passes, influence of the agitator speed.

Level of fill: 60%.

plane has an equal probability of reaching any point in the plane between the agitator shaft and the outer wall of the cylinder. The results of this calculation yield 36 mm, a value which is consistent with the asymptotic value seen in Figure 6b. However, this does not imply that the material is uniformly dispersed in the cross-sectional plane. Indeed, it is known not to be the case (Figure 2).

Figure 7 presents the local RMS_r in the cross-sectional plane based on tracer displacement after one blade rotation as a function of fill. For the calculation, the blade starts and ends out of the bulk so that the bed is initially and finally nearly at rest. The radial dispersion is not uniform. At 20% of fill (Figure 7a), the region where the radial mobility is the most intense is that situated just beneath the agitator shaft and is associated with the cascading process. The clearance region situated between the tip of the blade and the inside of the shell is one of low radial mobility. A region of slight radial dispersion is encountered as the blade enters the bed and remains present at all levels of fill. As the level of fill is increased, the region of intense radial motion remains in the middle of the cascading region and, at 60% fill, is found above the central shaft. A region of greater radial mobility where the blade leaves the bed becomes more pronounced as the level of fill is, say, 30% to 40%. This region is linked to the ready sliding material off the blade as it leaves the bed. At a level of fill of 50% to 60%, this region is submerged by a zone of lower mobility. The increased overburden of material then exerts a downward stress which pushes material off the blade towards the center of the mixer, hence, enhancing radial flow in this region.

Figure 8 presents RMS_r as a function of the number of blade passes for the four agitator speeds investigated at 60% fill. The radial displacement is only dependent on the number of blade passes and is independent of speed. In the range of agitator speeds investigated, RMS_r reaches the same asymptotic limit, close to the theoretical value of 36 mm mentioned earlier.

Axial Dispersion

Level of fill

A 1-D dispersive model may be used to describe axial particle mixing, assumed to be a random or stochastic process, that is, that particle motion obeys statistical laws and that there is no influence of the past motion of a particle on its future motion. A dispersion coefficient $\mathfrak{D}$, established by Einstein (1905) given by

$$\mathfrak{D} = \lim_{\Delta t \to 0} \frac{\langle \Delta x^2 \rangle}{2\Delta t} \tag{2}$$

is thus employed. Here, $\langle \Delta x^2 \rangle$ is the mean-square axial displacement considered during the time interval Δt. The motion of the tracer is tracked considering each data point P_i of the data file as a starting point; the subsequent axial displacement of the tracer is found after a time t. The square of the axial displacement for all the data points is then averaged and leads to the mean square of the axial displacement of the tracer MS_x for this time t.

MS_x was found to increase linearly with time for all levels of fill over small agitation times, typically 10 s, that is, approximately five blade rotations. For longer periods of agitation, end effects can no longer be ignored and MS_x would tend to a asymptotic limit since the system has finite axial dimensions. The theoretical limit of MS_x for a simple 1-D system of length L is $L^2/6$ (Bridgwater et al., 1993), giving a numerical value of 7×10^4 mm^2. Figure 9 presents the dispersion coefficient calculated employing Eq. 2. This rises from 15 mm^2/s for 20% of fill to attain a maximum of 23 mm^2/s for 40% of fill and then decreases to 7 mm^2/s for 60% of fill.

The existence of a maximum in axial dispersion can be explained by examining two phenomena. First of all, the amount of powder lifted by the blade increases with fill as observed

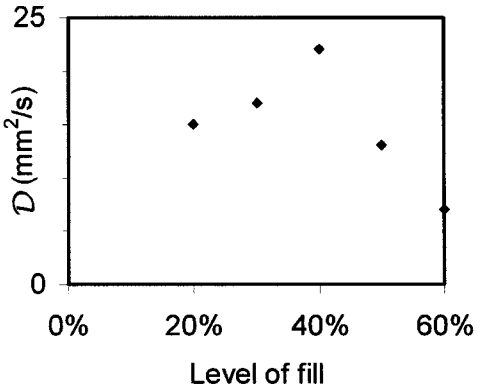

Figure 9. Influence of the level of fill on the axial dispersion coefficient $\mathcal{D}$; $N = 38$ rpm.

by Bagster and Bridgwater (1970), hence, increasing the probability for the powder to disperse in the space above the bed and on the free surface. Secondly, the area of the free surface and the volume of the open space above the bulk increase with fill up to 50% and then decrease. It then can be deduced that the interaction of these two phenomena varies as fill increases, leading to a maximum axial dispersion at about 40% of fill. Further investigations would be required to assess the validity of such a model.

Calculation of the axial dispersion coefficient as a function of position in the cross-sectional plane is reported in Figure 10. This shows the local axial dispersion coefficient calculated for a mixing time corresponding to a single blade rotation or 1.6 s for a rotation speed of 38 rpm. The initial blade position for the calculation was between 180° and 210° measured from the lower vertical position of the blade in the clockwise direction to ensure that the blade was initially out of the particle bed. The white bins represent those where the number of data points was insufficient (less than twenty) to calculate a local dispersion coefficient. At all levels of fill, the local dispersion coefficient is between five and ten times lower in the middle of the bed than that in the free surface region, showing that axial motion occurs preferentially near the free surface (Figure 10a). This remains true as the level of fill increases. At levels of fill between 30% and 50%, the powder flows increasingly over the rotating shaft; the free surface is then disturbed by the rotating shaft, and axial motion becomes more complex. At the highest level of fill (Figure 10e), the most marked axial motion occurs on the free surface above the shaft in the middle of the cascading region.

A region of higher dispersion coefficient appears near the wall corresponding to a blade position of 45° measured from the lower vertical position of the blade in the clockwise direction. A region of higher radial dispersion was observed in the same portion of the cross-sectional plane (Figure 6e). This may again be explained, as for radial dispersion, by material slipping off the blade as a result of the force exerted by the powder situated above the blade.

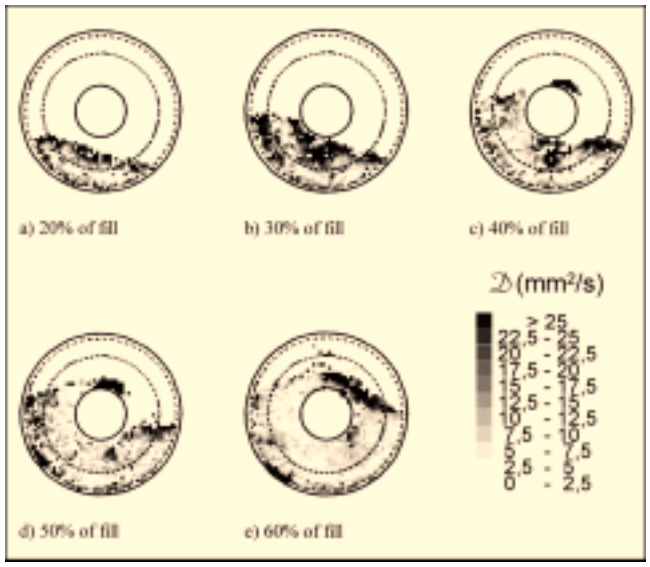

Figure 10. Axial dispersion coefficient $\mathcal{D}$ calculated in the cross-sectional view; $N = 38$ rpm.

The white bins are those where the number of data points was insufficient (less than twenty) to calculate a local dispersion coefficient.

Agitator speed

Axial mobility, characterized by the mean square of the axial displacement, increases linearly with the number of blade rotations (Figure 11) and varies little with speed. The dispersion coefficient increases linearly with speed as Figure 12 shows and corresponds to a dispersion coefficient of 9 mm^2/blade rotation. Thus, in the range of agitator speeds investigated, axial motion is independent of speed and is a function of the number of blade passes only, again consistent with the observations on transaxial flow reported above and the findings of Laurent et al. (2000). These findings are a direct consequence of low agitator speed implying that inertial effects can be neglected.

Conclusions

Reconstruction of the dispersion of three labeled portions of the transaxial plane showed two types of behavior as fill is increased. At low fill, the material is free to flow and to cas-

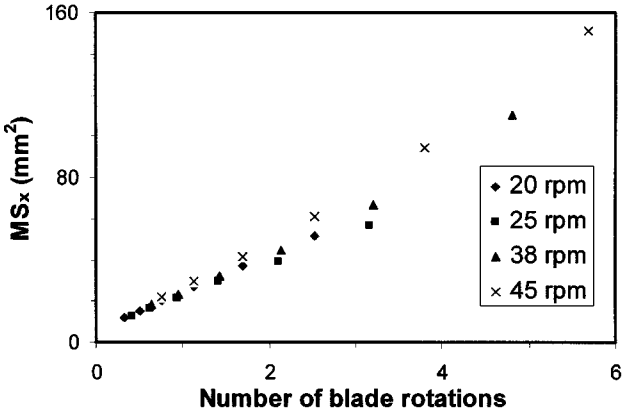

Figure 11. Mean square of the axial displacement MS_x vs. number of blade rotations, influence of the speed. Level of fill: 60%.

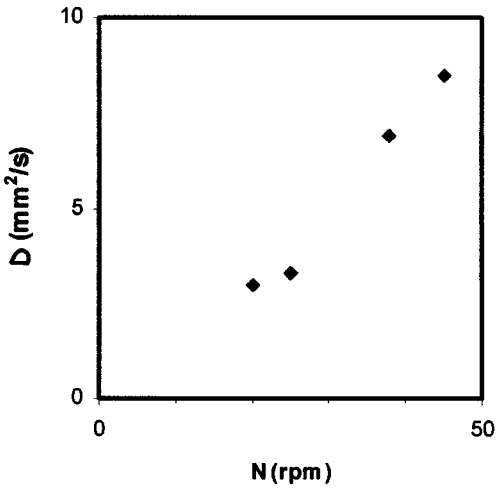

Figure 12. Influence of the agitator speed on the axial dispersion coefficient $\mathfrak{D}$.

Level of fill: 60%.

cade on the free surface. At high fill, the powder is pushed through the channel between the mixer shaft and the shell before reaching the free surface. One region lay in the clearance between the tip of the blade and the outer wall. Particle displacement was observed to increase with fill, probably because of increased particle-particle friction forces with increased level of fill. The second region lay in the central part of the bed beneath the agitator shaft. The deformation of a blob was found to be strongly affected by the presence of a circulation loop situated beneath the agitator shaft, thus inhibiting material dispersion. At high fill, the blob became less elongated as the powder is channeled between the agitator shaft and the outer cylinder wall. The third region lay in an annular section in the path of the blade. At low fill, the blob is lifted by the blade and falls in the space created behind the blade and becomes elongated. At high fill, the blob is also stretched and is pushed against the outer wall, due to increased body forces.

The radial and axial mobility were characterized by the root mean square of the radial displacement and by the axial dispersion coefficient, respectively. Regions of low and high radial displacement were found approximately in the same portions of the transaxial plane as those of axial displacement. Thus, radial and axial mobility were both found to be significantly higher both near the free surface and in the region below the top edge of the free surface when the blade is horizontal. The former is a result of particle-particle collisions in the open space above the bed and on the free surface. The latter arises since material slips off the blade towards the center of the mixer chamber as the blade rotates towards the free surface. The axial dispersion coefficient was found to be a maximum at around 40% of fill, the level of fill for which radial dispersion is also greatest. This probably linked to the flow experiencing a bifurcation, whereby material can flow either under the agitator shaft or over it, enhancing radial dispersion.

A parallel between experiments using a rotating drum may be drawn. Metcalfe et al. (1995) as well as McCarthy et al. (1995) observed a central static core forming as the level of fill increases. Here, the agitator shaft can be considered to be the central core as long as the fill level is above the top of the agitator shaft. One possible future development is to consider an extension of their approach using the understanding of the three transaxial regions investigated here. This could provide a step towards a scientific scale-up strategy.

For the range of agitator speeds studied nondimensional velocities, root mean square of the tracer radial displacement and nondimensional axial dispersion coefficients were not affected by speed. Thus, radial and axial flows are dictated by the number of blade passes as observed by Laurent et al. (2000). This is a significant finding for design purposes as it shows that mixing is achieved in relation to the total work input and not the instantaneous power.

This work opens the prospect of obtaining links between granular flow patterns and a wide range of operations such as heat transfer and chemical reaction since the data file carries information on exposure time distributions at such surfaces, on the free surface or in the gas space above the bed. Camera advances with increased spatial resolution may allow the high strain rates occurring in mixers for cohesive powders in agglomerators to be assessed. Thus there is strong reason to consider that the "Cinderella" subject of powder mixing, so vital to so many processes and products, is becoming accessible to an analysis based on engineering science.

Notation

$\mathfrak{D}$ = axial dispersion coefficient, mm^2/s
L = mixer length, mm
MS_x = mean square of the axial displacement of the tracer, mm^2
N = rate of rotation of agitator, rpm
RMS_r = root mean square of the radial displacement, mm
t = time, s
x = axial position of the tracer, mm

Acknowledgments

The authors would like to acknowledge the financial support provided by Elf. Thanks are also extended to D. J. Parker, D. Benton, and R. Forster of the Positron Imaging Centre in the School of Physics and Astronomy at the University of Birmingham for their technical support. The authors are also grateful to Dr. Silvana Cardoso for useful comments related to the section dealing with deformation of blobs.

Literature Cited

Bagster, D. F., and J. Bridgwater, "The Flow of Granular Material over a Moving Blade," *Powder Technol.*, **3**, 323 (1970).

Bridgwater, J., C. J. Broadbent, and D. J. Parker, "Study of the Influence of a Blade Speed on the Performance of a Powder Mixer using Positron Emission Particle Tracking," *Trans. IChemE*, **71**, 673 (1993).

Einstein, A., "Über die Bewegung Kleiner Partikel Suspendiert in Stillstandiger Flüssigkeit Gebunden mit Molekular-Kinetischer Theorie der Wärme" (Movement of Small Particles in a Stationary Liquid Demanded by the Molecular-Kinetic Theory of Heat), *Ann. Phys.*, **17**, 558 (1905).

Kaneko, Y., T. Shiojima, and M. Horio, "Numerical Analysis of Particle Mixing Characteristics in a Single Helical Ribbon Agitator using DEM Simulation," *Powder Technol.*, **108**, 55 (2000).

Khakhar, D. V., J. J. McCarthy, J. F. Gilchrist, and J. M. Ottino, "Chaotic Mixing of Granular Materials in 2D Tumbling Mixers," *CHAOS*, **9**, 195 (1999).

Laurent, B. F. C., J. Bridgwater, and D. J. Parker, "Motion in a Particle Bed Agitated by a Single Blade," *AIChE J.*, **46**, 1723 (2000).

Malhotra, K., A. S. Mujumdar, and M. Okazaki, "Particle Flow Patterns in a Mechanically Stirred Two-Dimensional Cylindrical Vessel," *Powder Technol.*, **60**, 179 (1990).
McCarthy, J. J., T. Shinbrot, G. Metcalfe, J. E. Wolf, and J. M. Ottino, "Mixing of Granular Materials in Slowly Rotated Containers," *AIChE J.*, **42**, 3351 (1995).
Metcalfe, G., and M. Shattuck, "Pattern Formation during Mixing and Segregation of Flowing Granular Materials," *Physica A*, **233**, 709 (1996).
Metcalfe, G., T. Shinbrot, J. J. McCarthy, and J. M. Ottino, "Avalanche Mixing of Granular Solids," *Nature*, **374**, 39 (1995).
Müller, W., and H. Rumpf, "Das Mischen von Pulvern in Mischern mit Axialer Mischebewegung," (Powder Mixing in Mixer with Axial Agitation), *Chem. -Ing. Tech.*, **39**, 365 (1967).
Ott, E., *Chaos in Dynamical Systems*, Cambridge University Press, Cambridge (1993).
Parker, D. J., C. J. Broadbent, P. Fowles, M. R. Hawkesworth, and P. McNeil, "Positron Emission Particle Tracking—a Technique for Studying Flow within Engineering Equipment," *Nucl. Instr. and Meth.*, **326**, 592 (1993).
Thornton, C., ed., "Numerical Simulations of Discrete Particle Systems," *Powder Technol.*, **109** (2000).
Williams, R. A., and C. G. Xie, "Tomographic Techniques for Characterising Particulate Processes," *Part. Part. Syst. Charact.*, **10**, 252 (1993).

Manuscript received Nov. 10, 2000, and revision received June 15, 2001.